Nanoparticle-based discrimination of single-nucleotide polymorphism in long DNA sequences.

María Sanromán-Iglesias,[†‡]Charles H. Lawrie,[‡‖] Luis M. Liz-Marzán,[†‖§]Marek Grzelczak,[†‖§*]

†CIC biomaGUNE, Paseo de Miramón 182, 20014 Donostia-San Sebastián, Spain

‡ Oncology Area, Biodonostia Research Institute, Donostia-San Sebastián, Spain

‖ Ikerbasque, Basque Foundation for Science, 48013 Bilbao, Spain

§ CIBER de Bioingeniería, Biomateriales y Nanomedicina, CIBER-BBN, 20014 Donostia-SanSebastián, Spain

KEYWORDS Spherical Nucleic Acid, Single-nucleotide polymorphism, gold nanoparticles, long sequences

ABSTRACT: Circulating DNA (ctDNA) and specifically the detection cancer-associated mutations in liquid biopsies promises to revolutionize cancer detection. The main difficulty however is that the length of typical ctDNA fragments (~150 bases) can form secondary structures potentially obscuring the mutated fragment from detection. We show that an assay based on gold nanoparticles (65 nm) stabilized with DNA (Au@DNA) can discriminate single nucleotide polymorphism in clinically-relevant ssDNA sequences (70-140 bases). The preincubation step was crucial to this process, allowing sequential bridging of Au@DNA, so that single base mutation can be discriminated, down to 100 pM concentration.

Detection of single nucleotide polymorphisms (SNP) in ssDNA sequences by selective aggregation of plasmonic nanoparticles carries the potential for rapid determination of cancer biomarkers in liquid biopsies such as blood.[1–3]Although, the detection of sequences of up to 40 bases without any signal amplification has been demonstrated[4,5] the average size of circulating DNA is ~150 bases in length,[6] and these longer fragments are more problematic as the increase of the sequence length affects the plasmon coupling (larger gaps between the particles), that decrease the limit of detection.[7] In addition, long DNA sequences form thermodynamically stable secondary structures that render the detection even more difficult.[8] Therefore, there is an obvious need for new solutions to detect long DNA sequences.

In earlier studies, we have reported a plasmonic assay comprising DNA-coated gold nanoparticles (AuNPs) that could discriminate SNP in less than 10 min.[9] Even though relatively large particles may lead to plasmon coupling upon aggregation, the assay is limited to the detection of rather short sequences (up to 23 bases). We report here that large plasmonic particles (65 nm) functionalized with modified DNA[10] can be used to detect single-base mutation in clinically relevant sequences with 140 bases in length. We found out that premixing the AuNPs (batch 1) with the target DNA was sufficient to induce aggregation upon addition of batch 2 (Figure 1b). In contrast, the addition of the target DNA to the mixture of two batches (standard sandwich assay, Figure 1a) had no effect on the aggregation.

As a target we choose the most common point mutation in non-small cell lung cancer (NSCLC), the L858R mutation that occurs in the Epidermal Growth Factor Receptor (EGFR) gene.[11] Detection of this mutation is an FDA and EMA-approved biomarker for the administration of TKI-therapy to NSCLC patients. Figure 1d-e show possible secondary structures of target sequences comprising 70 and 140 bases, with indication of the binding sites of Au@DNA and the location of a single-point mutation. As a signal transducer, we used AuNPs with 65 nm in diameter, stabilized by short sequences that were complementary to either a mutation-free region in the target DNA (WT) or to a region that contained a single-base mutation (MUT) (Figure 1c). Each AuNP was stabilised by ~1500 WT or MUT strands grafted to the surface via thiol groups, as determined by a fluorescence kit (see Supporting Information).

We first implemented a standard sandwich approach but found no effect on Au@DNA aggregation, meaning that the solution containing both Au@MUT and Au@WT remained stable upon the addition of target sequence (5 mM), in the presence of PBS and NaCl, as confirmed by UV-Vis and DLS characterisation (Figure S1). Aggregation is however possible by tailoring the incubation process (Figure 1b). Au@WT was preincubated with a target DNA (70 bases), either match or mismatch, for 1 h under constant shaking. Subsequent addition of the second Au@MUT batch led to selective aggregation within 3 hours. The concentration of target sequence was 5 nM, which translates into 380 copies of target DNA per NP. Figure 2a-b shows UV-Vis spectra at different times after addition of Au@MUT that is after addition of second batch. The localised surface plasmon resonance (LSPR) band is broadened suggesting more pronounced aggregation of the AuNPs in the presence of the match sequence than in the presence of the mismatch. By monitoring the aggregation degree ($R = Abs_{700}/Abs_{538}$), a difference of 0.4 was observed between match and mismatch sequences, after 1 hour of incubation, which increased up to 0.6 after 3 hours (Figure 2c). Importantly, our assay allows for a colorimetric detection of the single-based mutation (Figure S2). DLS measurements (Figure 2d) confirmed the trends observed by UV-Vis spectroscopy. The average diameter of the initial mixture in 1xPBS increased from 81

nm to 262 nm after 3 hours of incubation. For the mismatch sequence, a diameter increase of 18 nm was observed after 3 hours of incubation. In the case of the control (no target), the size remained constant.

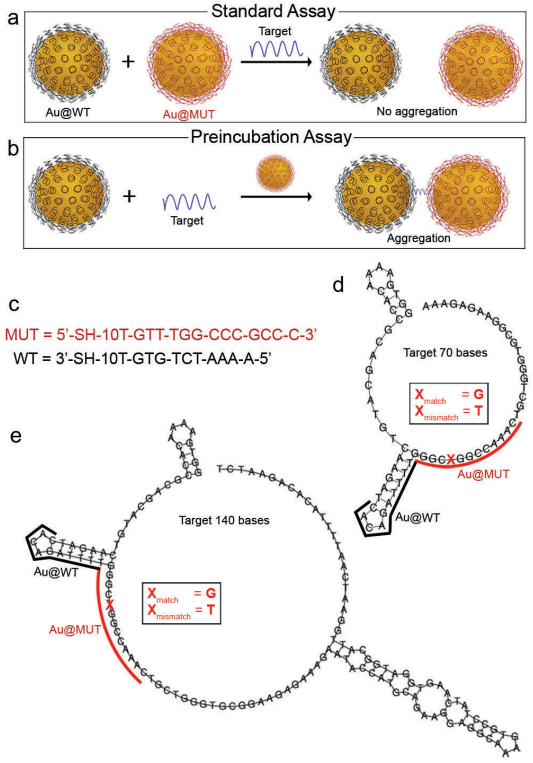

Figure 1. General description of the detection strategy. (a) Standard sandwich assay in which the addition of the long target DNA to the mixture of two different Au colloids has no effect on the aggregation. (b) Preincubation of one batch of nanoparticles with target DNA, followed by addition of a second batch leads to sensitive detection. (c) Selected sequence of DNA stabilising gold nanoparticles. (d,e) Possible secondary structures (Dynalign)[13]of the target sequences used in this study showing the complementary sequences to those on the nanoparticles and position of the mutation.

Next, we explored the performance of the assay for discrimination of a single-base mutation in even longer target DNA of 140 bases (Figure 2 e-h). The LSPR of the solution containing the match sequence decreased and broadened (Figure 2e). In the case of the mismatch sequence only a slight decrease of the plasmon band was observed (Figure 2f). Although the aggregation degree (Figure 2g) was similar (0.4) for match and mismatch sequences after one hour of incubation, the difference was more pronounced at longer incubation times (3h), clearly showing that specificity was lower for 140 long sequences as compared to the sequences containing 70 bases. The initial average diameter of the Au@DNA was 92 nm and increased to 158 nm after 3 hours (Figure 2h). For the mismatch sequence, the final diameter after 3 hours was 114 nm, whereas the particle size in the control experiment remained constant.

To further study the importance of the preincubation step, we reversed the order of pre-mixing. The target was first mixed with Au@MUT, and then Au@WT was added. Although selectivity toward SNP was indeed appreciated, the difference in aggregation degree was much lower as compared to the pre-incubation with Au@WT. For the target comprising 70 bases, we obtained R = 0.15 while for the target of 140 bases, we found R = 0.05 (Figure S3). Our observations clearly indicate that the target exhibits better accessibility when conjugated with Au@WT. Mirkin and coworkers[12] *have shown that the hybridization of ssDNA on the Au surface with short sequences extends the non-hybridized bases of ssDNA, making them more accessible to the incoming target sequence. Our observation suggests an analogous scenario in which the target, instead of the probe, undergoes a conformational change.*

Our essay shows high selectivity toward single-based mutation. It has been shown[14,15] that the discrimination of single-base mutations is related to the stability of the target molecule. In other words, longer targets are less discriminative with respect to point defects than shorter ones. It should be considered that a point defect in sequences containing 70 or 140 bases represents only 1.5 or 0.7 % of the complete sequence, respectively, making our assay a convenient strategy for detection of the mutation in long sequences.

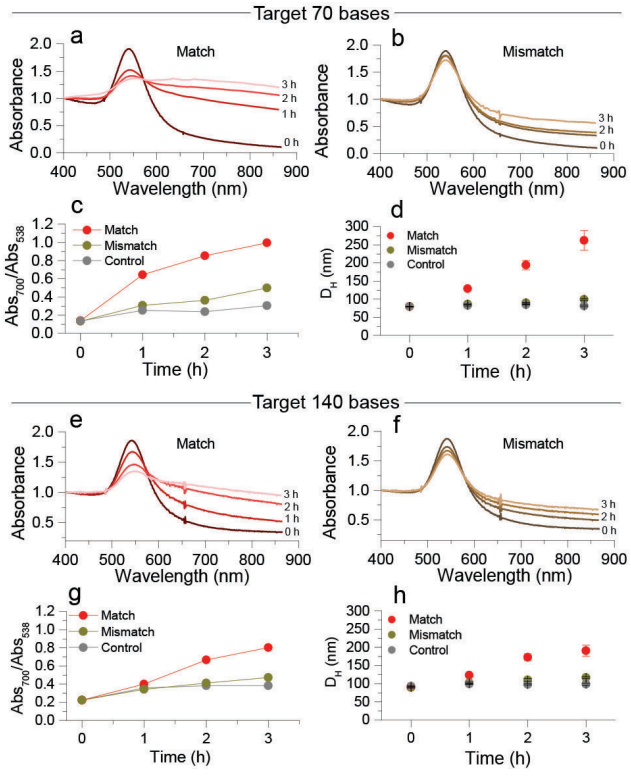

Figure 2. Selective discrimination of single –base mutation in a target DNA of 70 (a-d) and 140 (e-h) bases. (a,b) UV-Vis spectra of AuNPs in the presence of match (a) and mismatch (b) containing 70 bases (c) Aggregation rate for match, mismatch and control (no target). (d) DLS monitoring of the aggregation process in the presence of target (70 bases, 5 nM).(e-h) Selective discrimination of a single–base mutation in a target of 140 bases. (e,f) UV-Vis spectra of AuNPs in the

presence of match (e) and mismatch (f). (g) Aggregation rate for match, mismatch and control. (h) DLS characterisation of the aggregation process in the presence of target 140 bases, 5 nM.

To evaluate the sensitivity of the assay, we performed the aggregation experiments for both targets (70 and 140, match and mismatch) at the following concentrations: 5, 1, 0.1 and 0.01 nM. Figure 3 shows the discrimination of SNP in the target containing 70 bases down to 0.1 nM. On the other hand, the target of 140 bases allows for discrimination down to 5 nM. (Figure S4). By employing the above-described protocol with a preincubation step, we observed that indeed at low concentration the discrimination becomes feasible, however requiring longer detection times (5 hours).

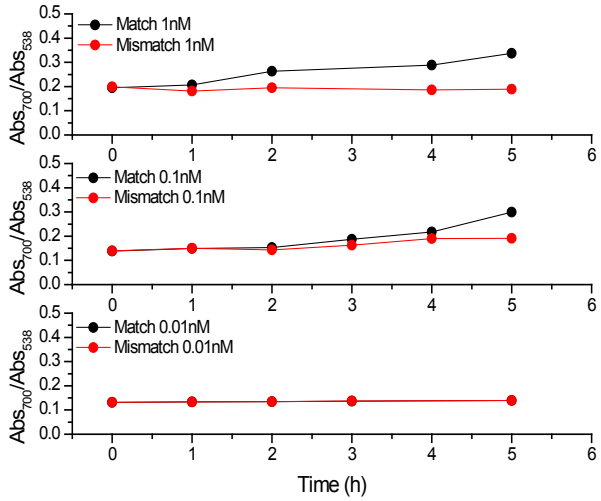

Figure 3. Selective discrimination of single–base mutation for a 70 bases target, in a concentration range from 1 nM to 0.01 nM.

To further determine to what extend the target molecules hybridize with WT or MUT during the preincubation step, we carried out a DLS analysis (Figure 4). Upon mixing of Au@WT with the match sequence, the hydrodynamic diameter increased from 93 to 104 nm and 106 nm for 70 and 140 bases, respectively, after one hour of incubation. On the other hand, the hydrodynamic diameter of Au@MUT increased from 86 to 89 nm (70 bases) and to 91 nm (140 bases). Note, that the initial hydrodynamic diameter of Au@MUT was 7 nm smaller as compared to Au@WT, owing to the different length and conformation of both sequences (see Figure 1c). The difference in the increase of hydrodynamic diameter for Au@WT (11 nm) and Au@MUT (2nm) upon incubation with the target sequence suggests that binding events on Au@DNA are sequence-dependent. Note that the incubation of either Au@WT or Au@MUT with a non-target sequence of 70 bases had no effect on the hydrodynamic diameter of the nanoparticles (Figure 4).

MUT and WT are complementary to different areas of the target (Figure 1) that initially can form a variety of secondary structures with multiple loops and hairpins. Upon hybridization, WT on AuNPs unbinds the secondary structure of the target, allowing the tail sequence to point toward the solution, and thereby increasing the hydrodynamic diameter. In the case of MUT, the same target molecule binds in the opposite direction, forcing the tail sequence to point toward the nanoparticles (Figure 4 and Figures S5-8). Both, the DLS analysis and the experiments of reversed pre-mixing (Au@MUT + target) suggest that the preincubation step disrupts the secondary structure. This reasoning is a basis for the statement that a preincubation step is crucial to open and stabilise the target molecules,[16] making the sequences more accessible toward binding events with Au@MUT in the second batch, thus facilitating the formation of the sandwich architecture.[12] In contrast, the target DNA exposed to both types of particles (standard assay) is unable to selectively bridge the two particle types within a reasonable time-scale. The competitive interaction of Au@WT and Au@MUT for the same target molecules constrains sterically the target in a stable coiled conformation.[17]

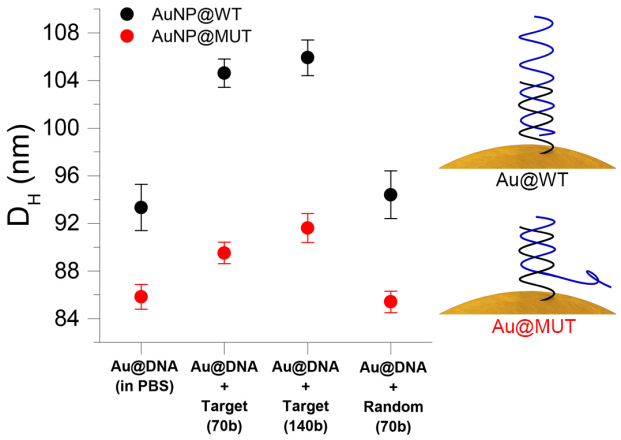

Figure 4. Hydrodynamic diameter, obtained by DLS, of either Au@WT or Au@MUT before and after incubation with the target sequences. The right-hand panel provides a schematic representation of the effect of preincubation on the increase in hydrodynamic diameter.

In conclusion, we showed a methodology to discriminate single-base mutation in long DNA sequences containing 70 or 140 bases. Preincubation of the target sequence with only one type of Au@DNA, facilitated the formation of a sandwich structure upon addition of the second type of Au@DNA and discriminate single-base mutation within one hour. Our approach suggest that spherical nucleic acids can disturb the secondary structure of long DNA sequences, making feasible the detection of relevant mutations in biological targets. As future directions, we foresee the use of the present assay in the detection of long sequences from dsDNA,[18] to study its validity in the detection of other mutations, and to decrease the discrimination time by varying the particle shape.

ASSOCIATED CONTENT

Supporting Information

The Supporting Information is available free of charge on the ACS Publications website.

Methods, UV-Vis-NIR spectra of standard assay, additional DLS data, secondary structures of DNA. (PDF)

AUTHOR INFORMATION

Corresponding Author

*E-mail: mgrzelczak@cicbiomagune.es

ACKNOWLEDGMENT

This work was supported by the Spanish Ministerio de Economía y Competitividad MINECO (grants: MAT2013-46101-R, MAT2013-49375-EXP) and FEDER funds (PI12/00663, PIE13/00048, DTS14/00109, PI15/00275)

REFERENCES

(1) Wu, Z., Jiang, P., Zulqarnain, H., Gao, H., and Zhang, W. (2015) Relationship between single-nucleotide polymorphism of matrix metalloproteinase-2 gene and colorectal cancer and gastric cancer susceptibility: a meta-analysis. *Onco Targets Ther 8*, 861–869.

(2) Antoniou, A. C., Casadei, S., Heikkinen, T., Barrowdale, D., Pylkäs, K., Roberts, J., Lee, A., Subramanian, D., De Leeneer, K., Fostira, F., Tomiak, E., Neuhausen, S. L., Teo, Z. L., Khan, S., Aittomäki, K., Moilanen, J. S., Turnbull, C., Seal, S., Mannermaa, A., Kallioniemi, A., Lindeman, G. J., Buys, S. S., Andrulis, I. L., Radice, P., Tondini, C., Manoukian, S., Toland, A. E., Miron, P., Weitzel, J. N., Domchek, S. M., Poppe, B., Claes, K. B. M., Yannoukakos, D., Concannon, P., Bernstein, J. L., James, P. A., Easton, D. F., Goldgar, D. E., Hopper, J. L., Rahman, N., Peterlongo, P., Nevanlinna, H., King, M.-C., Couch, F. J., Southey, M. C., Winqvist, R., Foulkes, W. D., and Tischkowitz, M. (2014) Breast-Cancer Risk in Families with Mutations in PALB2. *New Engl. J. Med. 371*, 497–506.

(3) Figl, A., Scherer, D., Nagore, E., Bermejo, J. L., Dickes, E., Thirumaran, R. K., Gast, A., Hemminki, K., Kumar, R., and Schadendorf, D. (2009) Single nucleotide polymorphisms in DNA repair genes XRCC1 and APEX1 in progression and survival of primary cutaneous melanoma patients. *Mutat. Res. Fund. Mol. Mech. Mut. 661*, 78–84.

(4) Guo, L., Xu, Y., Ferhan, A. R., Chen, G., and Kim, D.-H. (2013) Oriented Gold Nanoparticle Aggregation for Colorimetric Sensors with Surprisingly High Analytical Figures of Merit. *J. Am. Chem. Soc. 135*, 12338–12345.

(5) Hu, Y., Zhang, L., Zhang, Y., Wang, B., Wang, Y., Fan, Q., Huang, W., and Wang, L. (2015) Plasmonic Nanobiosensor Based on Hairpin DNA for Detection of Trace Oligonucleotides Biomarker in Cancers. *ACS Appl. Mater. Interfaces 7*, 2459–2466.

(6) Underhill, H. R., Kitzman, J. O., Hellwig, S., Welker, N. C., Daza, R., Baker, D. N., Gligorich, K. M., Rostomily, R. C., Bronner, M. P., and Shendure, J. (2016) Fragment Length of Circulating Tumor DNA. *PLOS Genetics 12*, e1006162.

(7) Jain, P. K., Huang, W., and El-Sayed, M. A. (2007) On the Universal Scaling Behavior of the Distance Decay of Plasmon Coupling in Metal Nanoparticle Pairs: A Plasmon Ruler Equation. *Nano Lett. 7*, 2080–2088.

(8) Rao, A. N., and Grainger, D. W. (2014) Biophysical properties of nucleic acids at surfaces relevant to microarray performance. *Biomater. Sci. 2*, 436–471.

(9) Sanromán-Iglesias, M., Lawrie, C. H., Schäfer, T., Grzelczak, M., and Liz-Marzán, L. M. (2016) Sensitivity Limit of Nanoparticle Biosensors in the Discrimination of Single Nucleotide Polymorphism. *ACS Sens. 1*, 1110–1116.

(10) Hurst, S. J., Lytton-Jean, A. K. R., and Mirkin, C. A. (2006) Maximizing DNA Loading on a Range of Gold Nanoparticle Sizes. *Anal. Chem. 78*, 8313–8318.

(11) Sharma, S. V., Bell, D. W., Settleman, J., and Haber, D. A. (2007) Epidermal growth factor receptor mutations in lung cancer. *Nat Rev Cancer 7*, 169–181.

(12) Prigodich, A. E., Lee, O.-S., Daniel, W. L., Seferos, D. S., Schatz, G. C., and Mirkin, C. A. (2010) Tailoring DNA Structure To Increase Target Hybridization Kinetics on Surfaces. *J. Am. Chem. Soc. 132*, 10638–10641.

(13) Reuter, J. S., and Mathews, D. H. (2010) RNAstructure: software for RNA secondary structure prediction and analysis. *BMC Bioinformatics 11*, 129.

(14) Naiser, T., Ehler, O., Kayser, J., Mai, T., Michel, W., and Ott, A. (2008) Impact of point-mutations on the hybridization affinity of surface-bound DNA/DNA and RNA/DNA oligonucleotide-duplexes: Comparison of single base mismatches and base bulges. *BMC Biotechnology 8*, 48.

(15) Suzuki, S., Ono, N., Furusawa, C., Kashiwagi, A., and Yomo, T. (2007) Experimental optimization of probe length to increase the sequence specificity of high-density oligonucleotide microarrays. *BMC Genomics 8*, 373.

(16) Chen, C., Wang, W., Ge, J., and Zhao, X. S. (2009) Kinetics and thermodynamics of DNA hybridization on gold nanoparticles. *Nucleic Acids Res 37*, 3756–3765.

(17) Zinchenko, A., Tsumoto, K., Murata, S., and Yoshikawa, K. (2014) Crowding by Anionic Nanoparticles Causes DNA Double-Strand Instability and Compaction. *J. Phys. Chem. B 118*, 1256–1262.

(18) Das, J., Ivanov, I., Sargent, E. H., and Kelley, S. O. (2016) DNA Clutch Probes for Circulating Tumor DNA Analysis. *J. Am. Chem. Soc. 138*, 11009–11016.

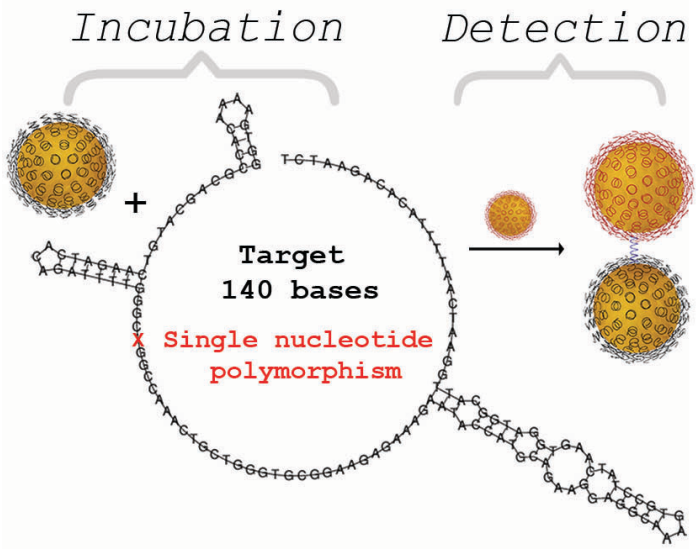

Insert Table of Contents artwork here